

Neutron Scattering Study of Colloidal Interactions in an Adsorbing Polymer Solution

X. Ye and P. Tong*

Department of Physics, Oklahoma State University, Stillwater, Oklahoma 74078

L. J. Fetters

Exxon Research and Engineering Company, Route 22 East, Annandale, New Jersey 08801

Received November 14, 1996; Revised Manuscript Received April 3, 1997[®]

ABSTRACT: Small-angle neutron scattering is used to study the interaction between the colloidal particles when they are suspended in an end-functionalized polymer solution. By matching the scattering length density of the solvent with that of the polymer, we measured the partial structure factor $S_c(Q)$ of the colloidal particles. The measurements reveal that the polymer molecules in the colloidal suspension partition themselves between the bulk solution and the adsorbed state. The free polymer molecules in the solution induce a depletion attraction between the colloidal particles, but the magnitude of the attraction is suppressed considerably by the adsorbed polymer chains on the colloidal surfaces. It is found that the measured $S_c(Q)$ can be well described by an effective interaction potential, which includes both the depletion attraction and the repulsion due to the polymer adsorption. The experiment demonstrates the effectiveness of using a polymer to control the colloidal interaction.

I. Introduction

Microscopic interactions between colloidal particles in polymer solutions control the phase stability of many colloid–polymer mixtures, which are of direct interest to industries. Lubricating oils and paint are examples of the colloid–polymer mixtures in which phase stability is desired. The interaction between the colloidal particles can be expressed in terms of an effective potential $U(r)$, which is the work required to bring two colloidal particles from infinity to a distance r in a given polymer solution. In the study of the interactions in mixtures of colloid and polymer, it is important to distinguish between polymers that are adsorbed on the colloidal surfaces and those that are free in solutions, because the two situations usually lead to qualitatively different effects.¹ When the polymer molecules are free in the solution, the interaction potential $U(r)$ can develop an attractive well because the polymer chains are expelled from the region between two colloidal particles when their surface separation becomes smaller than the size of the polymer chains.² This depletion effect leads to an unbalanced osmotic pressure difference pushing the colloidal particles together, which results in an effective attraction between the colloidal particles. If the attraction is large enough, phase separation occurs in the colloid–polymer mixture.^{3,4}

Recently, we have studied the depletion interaction in a mixture of a hard-sphere-like colloid and a nonadsorbing polymer (hydrogenated polyisoprene).^{5,6} By matching the scattering length density of the solvent with that of the polymer, we measured the colloidal (partial) structure factor $S_c(Q)$. It was found that the measured $S_c(Q)$ for different colloid and polymer concentrations can be well described by an effective interaction potential $U(r)$ for the polymer-induced depletion attraction between the colloidal particles. The magnitude of the attraction is found to increase linearly with the polymer concentration, but it levels off at higher polymer concentrations. This reduction in the depletion attraction can be explained by the screening of the

interaction between the polymer chains at high concentrations. The experiment demonstrates the effectiveness of using a nonadsorbing polymer to control the magnitude as well as the range of the interaction between the colloidal particles.

In this paper we report a small-angle neutron scattering (SANS) study of the interaction between the colloidal particles when they are suspended in an adsorbing polymer solution. In the experiment to be described below, we replace the nonadsorbing polymer with its single-end-functionalized derivative to modify the direct polymer–colloid interaction and see how the interparticle potential $U(r)$ changes when the polymer chains adsorb onto the colloidal surfaces. The polymer adsorption can modify the colloidal interaction in two ways. First, it reduces the number of free polymer chains in the solution, and therefore the magnitude of the depletion attraction is decreased. Second, the adsorbed polymer molecules in a good solvent resist the approach of other particles through a loss of their conformational entropy. Surfaces are then maintained at separations large enough to damp the attractions due to the depletion effect or London–van der Waals force, and the colloidal suspension is stabilized.⁷ In recent years many theoretical and experimental studies on the polymer adsorption have been carried out in various aqueous and organic colloidal suspensions.^{1,8} Most of the previous experiments, however, were restricted to examining the phase behavior and other thermodynamic properties of the colloid–polymer mixtures.^{9,10} While these phase measurements are useful in studies of macroscopic properties of the mixtures, they are much less sensitive to details of the molecular interactions in the system. Microscopic measurements, such as radiation-scattering experiments, therefore, are needed to directly probe the molecular interactions in the mixtures. With this knowledge, one can estimate the phase stability properties of the colloid–polymer mixtures in a straightforward way.

In contrast to the previous phase studies of the colloid–polymer mixtures,^{1,8–10} we have recently carried out a laser light scattering study of the interaction

* Author to whom correspondence should be addressed.

[®] Abstract published in *Advance ACS Abstracts*, June 15, 1997.

between the colloidal particles when they are suspended in adsorbing polymer solutions.¹¹ In the experiment, the second virial coefficient of the particles as a function of the polymer concentration was obtained from the measured concentration dependence of the scattered light intensity. The experiment demonstrated that the light-scattering technique is indeed capable of measuring changes of the colloidal interaction when the suspension medium is changed from a nonadsorbing polymer solution to an adsorbing one. However, the interpretation of the measurements was somewhat complicated by the unwanted scattering from the polymer. Assumptions were made in order to deal with the interference effect between the colloid and the polymer. In the present study, we use the SANS technique with isotopically mixed solvents to eliminate the undesirable scattering from the polymer and directly measure the colloidal (partial) structure factor $S_c(Q)$ over a suitable range of the scattering wavenumber Q . The measured $S_c(Q)$ is directly related to the interaction potential $U(r)$, and therefore it provides more detailed information about the colloidal interaction in the polymer solutions than the second virial coefficient does.

The colloidal particle chosen for the study consists of a calcium carbonate (CaCO_3) core with an adsorbed monolayer of a randomly branched calcium alkylbenzenesulfonate surfactant. Monodispersed hydrogenated polyisoprene (poly(ethylene-propylene) or PEP) and its single-end-functionalized derivative are used to modify the interaction between the colloid and the polymer. Both the polymer molecules and the colloidal particles are dispersed in a good solvent, decane. Such a non-aqueous colloid-polymer mixture is ideal for the investigation attempted here, since the colloidal suspension is approximately a hard-sphere system, and both the colloid and the polymer have been well characterized previously using various experimental techniques.^{5,6,12-17} Because the basic molecular interactions are tuned to be simple, the SANS measurements in the colloid-polymer mixtures can be used to critically examine the current theory for the polymer adsorption on colloidal surfaces.^{1,7,8}

The paper is organized as follows. In section II, we present the calculation of the colloidal structure factor $S_c(Q)$ using an interaction potential $U(r)$, which includes both the depletion attraction and the repulsion due to the polymer adsorption. Experimental details appear in section III, and the results are discussed in section IV. Finally, the work is summarized in section V.

II. Theory

In the experiment to be described below, we are interested in the partial structure factor, $S_c(Q)$, for the colloidal particles, and therefore the scattering length density of the solvent is chosen to be the same as that of the polymer. In this case, the polymer molecules become invisible to neutrons and the total scattered intensity from the colloid-polymer mixture can be written as^{18,19}

$$I(Q) = K_c^2 \rho_c P_c(Q) S_c(Q) \quad (1)$$

In the above, ρ_c is the number density of the colloidal particles, $P_c(Q)$ is their scattering form factor, and K_c is their scattering length density, which has taken into account the contrast between the particles and the solvent. The scattering wavenumber $Q = (4\pi/\lambda_0) \sin(\theta/2)$ with λ_0 being the wavelength and θ the scattering

angle. The structure factor $S_c(Q)$ measures the colloidal interaction and is proportional to the Fourier transform of the radial distribution function $g_c(r)$ for the particles. Hereafter, we will use the subscripts c and p to identify the colloid and the polymer, respectively. Experimentally, $S_c(Q)$ is obtained by

$$S_c(Q) = \frac{I(Q)}{K_c^2 \rho_c P_c(Q)} \quad (2)$$

where $K_c^2 P_c(Q)$ is the scattered intensity per unit concentration measured in a dilute pure colloidal suspension, in which the colloidal interaction is negligible and thus $S_c(Q) = 1$.

To calculate $S_c(Q)$, one needs to solve the Ornstein-Zernike equation for the direct correlation function $C(r)$ using a known interaction potential $U(r)$.²⁰ For hard-sphere-like particles in an adsorbing polymer solution, the effective interaction potential $U(r)$ can be written as

$$U(r) = \begin{cases} +\infty & r \leq \sigma \\ \delta U_d(r) + \delta U_a(r) & r > \sigma \end{cases} \quad (3)$$

where σ is the particle diameter, $\delta U_d(r)$ is the potential for the depletion attraction, and $\delta U_a(r)$ describes the repulsion due to the polymer adsorption. It has been shown that the depletion potential $\delta U_d(r)$ has the form^{2,21}

$$\delta U_d(r) = \begin{cases} -\Pi_p V_0(r) & \sigma < r \leq \sigma + 2R_g \\ 0 & r > \sigma + 2R_g \end{cases} \quad (4)$$

where R_g is the radius of gyration of the polymer molecules and Π_p is their osmotic pressure. The volume $V_0(r)$ of the overlapping depletion zones between the two colloidal particles is given by^{2,21}

$$V_0(r) = v_p \left(\frac{\lambda}{\lambda - 1} \right)^3 \left[1 - \frac{3}{2} \left(\frac{r}{\sigma \lambda} \right) + \frac{1}{2} \left(\frac{r}{\sigma \lambda} \right)^3 \right] \quad (5)$$

where v_p is the volume occupied by a polymer molecule and $\lambda = 1 + 2R_g/\sigma$.

The potential $\delta U_a(r)$ due to the polymer adsorption depends strongly on the conformation of the polymer chains attached to the colloidal surfaces. For a large flat surface, Alexander²² and de Gennes²³ have shown that the conformation of the adsorbed chains is determined by the polymer surface coverage ζ . For small values of ζ , the adsorbed chains do not overlap, and each of them occupies roughly a half-sphere with a radius comparable to R_g . At high surface coverage, however, the end-grafted polymer chains overlap and are strongly stretched along the direction normal to the surface to avoid a high monomer density. The grafted chains thus form a "brush", and their configurations are quite different from those of free polymer chains in a solution.^{24,25} For the two limiting surface coverages, elegant and relatively simple theoretical models have been developed to describe the interaction between two parallel plates covered with the adsorbed polymer chains.²⁴⁻²⁷ To apply the theoretical results to the colloidal interactions in an adsorbing polymer solution, one needs to consider two more complications in the experiment. First, the colloidal surfaces are curved, and an equation is needed to relate the calculated interaction free energy between two planar surfaces to the measured force (and hence the interaction potential) between two spherical particles. The equation can be

obtained under the Derjaguin approximation, which is valid only when the range of the interaction is much smaller than the radius of the spheres.²⁸ In a recent experiment, Gee et al.,²⁹ compared the direct force measurements between two macroscopic surfactant-coated mica surfaces separated by an organic liquid with the light-scattering measurements of the interaction potential in an analogous colloidal suspension (i.e., the colloidal particles were coated with the same surfactant and dispersed in the same medium). Excellent agreement between the two independent measurements was found in a system where the interaction potential was modulated by small organic molecules. In this case, the interaction range is small compared with the particle size and the Derjaguin approximation is expected to be applicable. For the colloid–polymer mixtures used in this experiment, however, the range of the polymer-induced interactions is on the order of the polymer radius of gyration, R_g , which is comparable with the particle size. In this case, the applicability of the Derjaguin approximation remains to be checked, and we will compare our scattering results with the recent direct force measurements³⁰ in a similar system in section IV.

The second complication is that in the colloid–polymer mixtures the polymer molecules partition themselves between the bulk solution and the adsorbed state. The amount of the polymer adsorbed on the colloidal surfaces depends on the polymer concentration and the free energy of adsorption.¹¹ In many cases, the polymer surface coverage ζ is not a known parameter and may lie in between the two extreme limits at which relevant theoretical results are available. In our previous studies of the colloidal mixtures with both the unfunctionalized and end-functionalized PEP,^{5,6,11,18} we have found that the interaction between the colloid and the PEP chain is repulsive. The polar end-group on the end-functionalized PEP was found to interact attractively with the polar core of the colloidal particles. The attractive adsorption energy was estimated to be approximately $4k_B T$. The amount of the polymer adsorbed on the colloidal surfaces was small, because the surfactant corona around the colloidal particles could mitigate the colloid–polymer interaction. To obtain the potential $\delta U_a(r)$ for this weakly adsorbing system, we now invoke the free energy calculation of Dolan and Edwards²⁷ for a single polymer chain confined in between two parallel plates separated by a distance z . It is assumed in the calculation that the polymer chains attached to a surface do not overlap with the neighboring chains and that only one end of the chain is attached to one of the planar surfaces. The triangles in Figure 1 show the calculated free energy $f(z)$ for large values of z , and the circles are for small values of z . In the plot the calculated $f(z)$ has been scaled by the thermal energy $k_B T$. It is seen from Figure 1 that $f(z)$ can be well approximated by a simple exponential function $f(z)/k_B T = 75e^{-2z/R_g}$ (the solid line), when z/R_g is in the range $0.5 < z/R_g < 5$.

Under the Derjaguin approximation,²⁸ one can relate the free energy $f(z)$ with the interaction force $F(r)$ between two equal spheres of diameter σ separated by a distance r . Therefore, we have

$$F(r) = \pi\sigma n_a k_B T f(r - \sigma) = 75\pi\sigma n_a k_B T e^{-2(r-\sigma)/R_g} \quad (6)$$

where n_a is the number of the adsorbed polymer chains per unit area. To get eq 6, we have assumed that, in the weak adsorption limit, the polymer chains attached

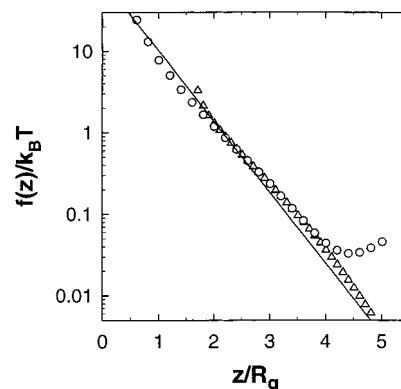


Figure 1. Calculated free energy $f(z)/k_B T$ by Dolan and Edwards for a single polymer chain confined in between two parallel plates separated by a distance z . The triangles show the calculated $f(z)/k_B T$ for large values of z , and the circles are for small values of z . The solid line is the exponential function $f(z)/k_B T = 75e^{-2z/R_g}$.

to one surface do not overlap with those on the opposite surface, and therefore the free energy change for compressing the two surfaces both covered with end-grafted polymer chains is increased by a factor of 2. The interaction potential $\delta U_a(r)$ between the two spheres then takes the form

$$\delta U_a(r) = \int_r^\infty F(r') dr' = P_a k_B T e^{-2(r-\sigma)/R_g} \quad (7)$$

where $P_a = 75\omega_a R_g/(2\sigma)$ with ω_a being the number of the adsorbed polymer chains per colloidal particle. Note that the characteristic range for the repulsive interaction is $R_g/2$.

As shown in eq 3, the total interaction potential $U(r)$ is composed of a hard core potential plus a weak perturbation $\delta U_d(r) + \delta U_a(r)$. In this case, the direct correlation function $C(r)$ can be obtained under the mean spherical approximation (MSA), which is a perturbative treatment to the Percus–Yevick equation.²⁰ Under MSA, we have

$$C(r) = \begin{cases} C_{HS}(r) & r \leq \sigma \\ -[\delta U_d(r) + \delta U_a(r)]/(k_B T) & r > \sigma \end{cases} \quad (8)$$

where $C_{HS}(r)$ is a known direct correlation function for the hard sphere system.^{31,32} Note that $C(r)$ is composed of three parts. (i) The hard core interaction involves the particle diameter σ and its volume fraction ϕ_c . (ii) The depletion attraction is described by the dimensionless amplitude $P_d = \Pi_p v_p/(k_B T)$ and the range parameter $\lambda = 1 + 2R_g/\sigma$. (iii) The repulsive interaction due to the polymer adsorption is characterized by the dimensionless amplitude $P_a = 75\omega_a R_g/(2\sigma)$ and the same range parameter λ .

With eq 8 one can calculate the Fourier transform of $C(r)$

$$\begin{aligned} C(Q) &= \int_0^\sigma C_{HS}(r) e^{-iQ \cdot r} dr + \int_\sigma^\infty \frac{-\delta U_d(r)}{k_B T} e^{-iQ \cdot r} dr + \\ &\quad \int_\sigma^\infty \frac{-\delta U_a(r)}{k_B T} e^{-iQ \cdot r} dr \\ &= C_{HS}(Q) + C_d(Q) + C_a(Q) \end{aligned} \quad (9)$$

The functional forms for $C_{HS}(Q)$ and $C_d(Q)$ have been given in ref 6, and $C_a(Q)$ has the form

$$\rho_c C_a(Q) = -\frac{6\phi_c P_a (\lambda - 1)^2}{Q\sigma [4 + (QR_g)^2]} \left[\left(\frac{2\sigma}{R_g} + \frac{4 - (QR_g)^2}{4 + (QR_g)^2} \right) \sin(Q\sigma) + \left(Q\sigma + \frac{4QR_g}{4 + (QR_g)^2} \right) \cos(Q\sigma) \right] \quad (10)$$

In the above, $\phi_c = \pi\rho_c\sigma^3/6$ is the colloid volume fraction. With the calculated $C(Q)$, we obtain the structure factor $S_c(Q)$ via the well-known relation²⁰

$$S_c(Q) = \frac{1}{1 - \rho_c C(Q)} \quad (11)$$

III. Experimental Section

The colloidal particles used in the experiment consisted of a calcium carbonate (CaCO_3) core with an adsorbed monolayer of a randomly branched calcium alkylbenzenesulfonate surfactant. These colloidal particles were supplied by Exxon Chemical Ltd. and have been well characterized previously using SANS and small-angle X-ray scattering (SAXS) techniques.^{12–14} The molecular weight of the particle was $M_c = 300\,000 \pm 15\%$ which was obtained from a sedimentation measurement.¹⁸ The colloidal samples were prepared by diluting known amounts of the concentrated suspension with the solvent, decane. The samples were then centrifuged at an acceleration of 10^8 cm/s^2 (10^5 g) for 2.5 h to remove colloidal aggregates and dust. The resulting suspension samples were found to be relatively monodispersed with an average hydrodynamic radius of $R_h = 5 \text{ nm}$ and $\sim 10\%$ standard deviation, as determined by dynamic light scattering.¹⁸ Our recent SANS and SAXS measurements^{5,6} revealed that the particle has a core radius of $R_0 = 2.0 \text{ nm}$ and a surfactant monolayer thickness of $\delta = 2.0 \text{ nm}$.

The polymers used in the study were hydrogenated polyisoprene (poly(ethylene-propylene) or PEP) and its single-end-functionalized derivative (amine-PEP), which were synthesized by an anionic polymerization scheme.^{15,16} The end-functionalized derivative contains a tertiary amino group capped at one end of the chain. The parent PEP and its end-functionalized derivative are model polymers ($M_w/M_n < 1.1$), which have been well characterized previously using various experimental techniques.^{15–17} The molecular weights (M_p) of the PEP and the amine-PEP were 26 000 and 25 000, respectively. Decane was used as the solvent because it is a good solvent for both the colloid and the polymers. Our recent scattering experiments^{5,6,11,18} revealed that the pure amine-PEP-decane solution behaves the same as the PEP-decane solution with no association found in the amine-PEP-decane solution. These experiments also showed that the unfunctionalized PEP chains do not adsorb onto the colloidal surfaces, whereas the polar end-groups on the amine-PEP chains interact attractively with the polar cores of the colloidal particles. It was found that the amine-PEP chains partition themselves between the bulk solution and the adsorbed state. Because of the surfactant corona around the colloidal cores, the polymer adsorption is mitigated and only a small amount of the polymer is adsorbed on the colloidal surfaces. Our recent SANS measurements^{5,6} showed that the polymer chains have a radius of gyration $R_g = 8.3 \text{ nm}$ and their second virial coefficient $A_2 M_p = 44.4 \text{ (cm}^3/\text{g)}$. With the measured A_2 one can define a thermodynamic radius (an effective hard-sphere radius) R_T via $4(4\pi/3)R_T^3 = A_2 M_p^2$. Thus we have $R_T = 4.85 \text{ nm}$, which is comparable with the radius of the colloidal particles.

The SANS measurements were performed at the High Flux Beam Reactor at Brookhaven National Laboratory. The incident neutron wavelength $\lambda_0 = 7.05 \pm 0.4 \text{ \AA}$, and the usable Q -range was $0.007 \text{ \AA}^{-1} \leq Q \leq 0.15 \text{ \AA}^{-1}$. All the scattering measurements were conducted at room temperature. The scattering cells were made of quartz and had a path length of 1 mm. The raw scattering intensity $I_r(Q)$ was measured by a

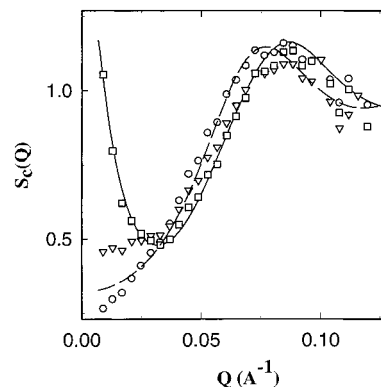


Figure 2. Measured colloidal structure factor $S_c(Q)$ for the pure colloidal suspension (\circ), the colloid-amine-PEP mixture (∇), and the colloid-PEP mixture (\square). The three samples have the same colloid concentration of $\rho'_c = 26.2 \text{ wt } \%$, and the two mixture samples have the same polymer concentration of $\rho'_p = 0.024 \text{ g/cm}^3$. The solid curve is a fit by eq 11 using the direct correlation function $C(Q)$ in eq 9 with $C_a(Q) = 0$. The dashed curve shows the fit of the hard sphere model to the circles.

two-dimensional detector. The corrected intensity, $I(Q)$, was obtained by applying the standard corrections due to the background scattering, solvent scattering, and sample turbidity via

$$I(Q) = \frac{I_r(Q) - I_b(Q)}{T_r} - \frac{I_s(Q) - I_b(Q)}{T_s} \quad (12)$$

and subsequently computing the azimuthal average. In the above, $I_b(Q)$ is the background scattering when the neutron beam is blocked, $I_s(Q)$ is the scattered intensity from the solvent, and T_r and T_s are the transmission coefficients of the scattering sample and the solvent, respectively. To eliminate the inhomogeneity of the detector's sensitivity at different pixels, we normalized the scattering data with an isotropic scattering standard. Because both decane and the polymer samples are protonated, the polymer chains in the mixture are invisible to neutrons. The colloidal structure factor $S_c(Q)$ was then obtained by using eq 2.

IV. Results and Discussion

To reduce the fitting ambiguity and to see how the colloidal interaction responds to the incorporation of the functional group on the polymer chains, we prepared two identical series of colloidal mixture samples, one with the PEP and other with the amine-PEP. For each series of the samples, the colloid concentration was kept the same and the polymer concentration ρ'_p was increased from 0.004 to 0.07 g/cm^3 . In this way the colloidal parameters in the mixture samples remain unchanged, and one can clearly see the effect of adding different polymers to the colloidal suspension. Figure 2 compares the measured $S_c(Q)$ for the colloid-amine-PEP mixture (triangles) with those for the pure colloidal solution (circles) and the colloid-PEP mixture (squares). The three samples have the same colloid concentration of $\rho'_c = 26.2 \text{ wt } \%$ and the two mixture samples have the same polymer concentration of $\rho'_p = 0.024 \text{ g/cm}^3$. Notable changes are found in the measured $S_c(Q)$, and their physical meaning becomes clear once we understand the scattering data from the pure colloidal solution and the nonadsorbing colloid-PEP mixture. The dashed curve in Figure 2 shows the fit to the pure colloid data by the simple hard sphere model,³³ which can be obtained by taking $C_a(Q) = C_d(Q) = 0$ in eq 9. In the fitting σ is found to remain constant for different colloid concentrations, and its best fit value is $\sigma = 7.7 \text{ nm}$. This value is very close to the measured particle size, $2(R_0$

+ δ) = 8.0 nm. Because the surfactant shell of the colloidal particle is somewhat "soft", we expect its effective hard shell thickness to be slightly smaller than δ . It is seen from Figure 2 that the hard sphere model fits the data well, except in the small- Q region. Since the measured $S_c(0)$ is smaller than the hard sphere value, the deviation in the small- Q region can be attributed to a weak repulsion between the soft surfactant shells.^{5,6} The small deviation in the low- Q region can be modeled by introducing a repulsive tail in the hard sphere potential $U(r)$ (see eq 3). The corresponding structure factor $S_c(Q)$ then can be obtained under the mean spherical approximation, as discussed in section II. Detailed fitting results for the pure colloidal samples have been given in refs 5 and 6.

Our recent SANS measurements^{5,6} have shown that the measured $S_c(Q)$ for the colloid-PEP mixture can be well described by the depletion potential $\delta U_d(r)$ in eq 4. It is seen from Figure 2 that the main effect of adding PEP is to increase the value of $S_c(Q)$ in the small- Q region, whereas the large- Q behavior of $S_c(Q)$ does not change much. We have found from the recent SANS measurements^{5,6} that the effect of adding PEP becomes more pronounced when the polymer concentration is further increased. Since $S_c(0)$ is proportional to the isothermal (osmotic) compressibility of the colloidal solution, an increasing $S_c(0)$ with ρ'_p indicates an increase in the attraction between the colloidal particles. The solid curve in Figure 2 shows the fit by eq 11 using the direct correlation function $C(Q)$ in eq 9 with $C_a(Q) = 0$. There are four parameters in the fitting. The colloid volume fraction ϕ_c and the diameter σ describe the hard core potential. The interaction amplitude $P_d = \Pi_p v_p / (k_B T)$ and the range parameter λ are for the attractive tail. In the fitting, the values of σ and ϕ_c are taken to be approximately the same as those obtained directly from the corresponding pure colloidal solution. The fitted λ is found to remain constant for different colloid and polymer concentrations, and its best fit value is $\lambda = 2.9$. This value is very close to the calculated $\lambda = 1 + R_g/(R_0 + \delta) = 3.07$. With the three fitting parameters fixed, we were able to fit all the scattering data from the colloid-PEP mixtures with only one free parameter, the interaction amplitude P_d . Detailed fitting results for the colloid-PEP mixture samples have been given in refs 5 and 6.

With the above understanding of the scattering data from the pure colloidal solution and the nonadsorbing colloid-PEP mixtures, we can qualitatively explain many new features of the scattering data from the colloid-amine-PEP mixtures by direct comparison prior to the detailed curve-fitting. As shown in Figure 2, the value of the measured $S_c(Q)$ in the small- Q region for the colloid-amine-PEP mixture lies in between those of the corresponding pure colloidal solution and the colloid-PEP mixture. Figure 2 thus reveals that the polymer-induced attraction in the colloid-amine-PEP mixture is reduced considerably when compared with the colloid-PEP mixture. The suppression of the depletion attraction is caused by the partial adsorption of the amine-PEP chains onto the colloidal surfaces. Because the interaction between the colloid and the unfunctionalized PEP is repulsive,¹⁸ the adsorption of the amine-PEP has to occur through the functional end group interacting attractively with the polar core of the colloidal particles. While the depletion interaction is reduced considerably in the colloid-amine-PEP mixture, there is still some residual attraction between the

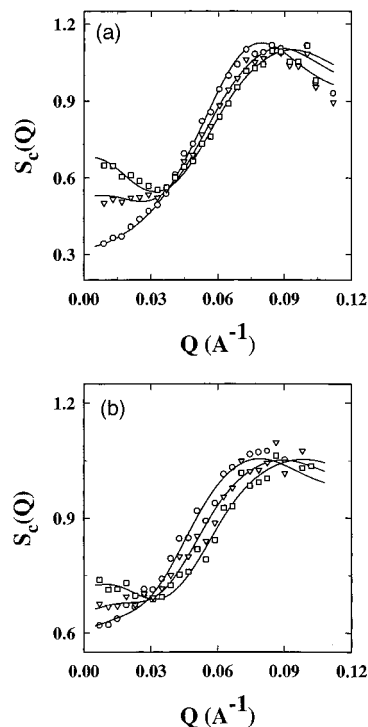


Figure 3. Measured colloidal structure factor $S_c(Q)$ of the colloid-amine-PEP mixture for three different polymer concentrations when (a) $\rho'_c = 26.2$ wt % and (b) $\rho'_c = 13.1$ wt %. The polymer concentrations (g/cm³) in (a) are as follows: 0.009 (○), 0.032 (▽), and 0.052 (□). Those in (b) are as follows: 0.016 (○), 0.030 (▽) and 0.049 (□). The solid curves are the fits by eq 11 using the direct correlation function $C(Q)$ given in eqs 9 and 10.

colloidal particles in the mixture when compared with the pure colloidal solution. This attraction is due to the unadsorbed free polymer molecules in the solution. As mentioned in section I, the adsorbed polymer chains can stabilize the colloid-polymer mixture. This effect was indeed observed in a simple phase study, in which we prepared two identical colloidal mixtures: one with the PEP and the other with the amine-PEP. The two samples have the same colloid concentration of 9.0 wt % and the same polymer concentration of 5.3 wt %. It was observed that the colloid-PEP mixture sample became phase separated with a visible interface, which separated the dark-brown colloid-rich lower phase from the light-brown colloid-poor upper phase. This is expected for the depletion effect.^{5,6} The colloid-amine-PEP mixture sample, on the other hand, was clear, and no sign of phase separation was observed.

To further study the effect of the polymer adsorption, we measured $S_c(Q)$ of the colloid-amine-PEP mixtures at different colloid and polymer concentrations. Figure 3 shows the measured $S_c(Q)$ for three different values of ρ'_p when (a) $\rho'_c = 26.2$ wt % and (b) $\rho'_c = 13.1$ wt %. It is seen that while the value of the measured $S_c(Q)$ in the small- Q region is smaller than that of the corresponding colloid-PEP mixture, it still increases with ρ'_p . This is a characteristic feature for the polymer-induced depletion attraction and has been observed in the colloid-PEP mixture samples.^{5,6} Figures 2 and 3 thus suggest that the end-functionalized PEP molecules in the colloidal solution partition themselves between the bulk solution and the adsorbed state. The free polymer molecules in the solution give rise to a depletion attraction between the colloidal particles, but the magnitude of the attraction is reduced considerably by the adsorbed polymer chains on the colloidal surfaces. This

Table 1. Fitting Results from Two Series of the Colloid–Amine–PEP Mixture Samples (a) and (b)

sample	ρ'_p (g/cm ³)	ϕ_p	ϕ_c	σ (nm)	λ	P_d	P_a	$(\phi_p)_a$
(a) $\rho'_c = 26.2$ wt %								
1	0.0	0.0	0.146	7.8	2.9	-0.1	0.0	0.0
2	0.009	0.506	0.135	7.5	2.9	0.022	0.106	0.205
3	0.017	0.947	0.125	7.3	2.9	0.105	0.201	0.355
4	0.024	1.338	0.115	7.1	2.9	0.16	0.284	0.462
5	0.032	1.758	0.110	6.7	2.9	0.21	0.373	0.580
6	0.039	2.189	0.102	6.6	2.9	0.25	0.441	0.637
7	0.052	2.872	0.100	6.3	2.9	0.28	0.441	0.625
8	0.070	3.889	0.098	5.9	2.9	0.334	0.441	0.612
(b) $\rho'_c = 13.1$ wt %								
1	0.0	0.0	0.063	7.7	2.9	-0.04	0.0	0.0
2	0.016	0.893	0.067	7.4	2.9	0.09	0.189	0.180
3	0.023	1.263	0.065	6.6	2.9	0.12	0.267	0.246
4	0.030	1.676	0.063	6.5	2.9	0.17	0.355	0.317
5	0.038	2.082	0.063	6.2	2.9	0.20	0.441	0.394
6	0.049	2.741	0.063	5.9	2.9	0.24	0.441	0.394

conclusion is also supported by our previous light-scattering study of the same system.¹¹ To further study the colloidal interaction in the adsorbing polymer solution, we use the model potential $U(r)$ given in eq 3 to fit the scattering data. The solid curves in Figure 3 show the fits by eq 11 with the direct correlation function $C(Q)$ given in eqs 9 and 10. There are five parameters in the fitting. The parameters ϕ_c , σ , P_d , and λ have been introduced in the study of the depletion interaction in the colloid–PEP mixture (see the discussion on Figure 2). The only extra parameter for the colloid–amine–PEP mixture is P_a , which describes the repulsive interaction due to the polymer adsorption. The fitting results are summarized in Table 1.

It is seen from Table 1 that the fitted λ remains constant for all values of ρ'_c and ρ'_p , and its best fit value $\lambda = 2.9$ is the same as that obtained from the colloid–PEP mixtures.^{5,6} For a fixed colloid concentration, the fitted particle diameter σ is found to decrease progressively with increasing polymer concentration. This behavior was also observed in the nonadsorbing colloid–PEP mixture. Figure 4a shows the fitted σ as a function of ϕ_p for the colloid–PEP mixtures with $\rho'_c = 17.5$ wt % (circles) and $\rho'_c = 8.7$ wt % (triangles). Here the effective polymer volume fraction ϕ_p is given by $\phi_p = \rho'_p/\rho^*$ with $\rho^* = M_p/[(4\pi/3)R_g^3]$ being the polymer overlap concentration. It is seen from Figure 4a that the fitted σ remains constant for small values of ϕ_p and then it starts to decrease with increasing polymer concentration. This decrease in particle diameter can be attributed to the contraction of the soft surfactant layer around the solid CaCO₃ core under the osmotic pressure of the polymer solution. In a recent theoretical study of the interactions between two parallel plates, both covered with a dense layer of terminally anchored polymer chains in equilibrium with a nonadsorbing polymer solution, Gast and Leibler³⁴ have shown that when the free polymer concentration ϕ_p is large enough, the steric polymer layer contracts under the osmotic pressure of the solution until its concentration exceeds that of the polymer solution. The data shown in Figure 4a agree qualitatively with their prediction. To find how the particle diameter σ changes with ϕ_p , one needs to calculate the free energy of the surfactant layer around the colloidal core. Unfortunately, this calculation is not available for our particles. Perhaps one can estimate the free energy of the surfactant layer using the recent calculation for a polymer brush by Milner et al.^{24,35}

Figure 4b shows the fitted σ as a function of the free polymer concentration $\phi_p - (\phi_p)_a$ in the solution for the

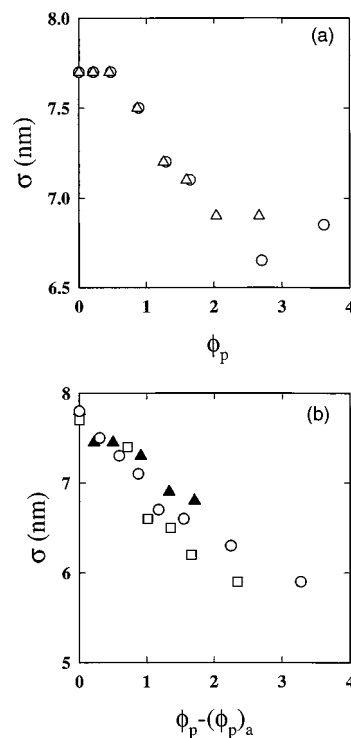


Figure 4. (a) Fitted particle diameter σ as a function of ϕ_p for the colloid–PEP mixtures with $\rho'_c = 17.5$ wt % (circles) and $\rho'_c = 8.7$ wt % (triangles). (b) Fitted σ as a function of $\phi_p - (\phi_p)_a$ for the colloid–amine–PEP mixtures with $\rho'_c = 26.2$ wt % (circles) and $\rho'_c = 13.1$ wt % (squares). The solid triangles are the fitted σ for the colloid–PEP mixture with $\rho'_c = 26.2$ wt %.

colloid–amine–PEP mixtures with $\rho'_c = 26.2$ wt % (circles) and $\rho'_c = 13.1$ wt % (squares). (We will discuss how the effective volume fraction $(\phi_p)_a$ occupied by the adsorbed chains is determined in the colloid–amine–PEP mixture below.) For comparison, we also plot the fitted σ for the colloid–PEP mixture with $\rho'_c = 26.2$ wt % (solid triangles). It is seen that the fitted σ for the colloid–amine–PEP mixtures decreases approximately in the same way as that for the nonadsorbing colloid–PEP mixture. Figure 4b thus suggests that the change in σ is not related to the polymer adsorption. In fact, one can directly see the change of σ from the measured $S(Q)$, because its first peak position is determined mainly by σ . As shown in Figure 2, the peak position of the measured $S(Q)$ for the two mixture samples is equally shifted toward a large- Q value (smaller σ) when compared with that for the pure colloidal solution. The amount of the shift is found to increase with the polymer concentration, as clearly depicted in Figure 3. From Figures 2–4 we conclude that, in both the functionalized and unfunctionalized PEP solutions, the size of the colloidal particle is shrunk due to the contraction of its soft surfactant layer under the osmotic pressure of the polymer solution. The amount of the decrease in σ depends on the free polymer concentration in the solution and is not very sensitive to the polymer adsorption. Because of the decrease in σ , the fitted colloid volume fraction ϕ_c is also found to decrease progressively with increasing polymer concentration. This behavior was observed in both the colloid–amine–PEP mixture and the colloid–PEP mixture.^{5,6} It should be mentioned that the fact that the size of the surfactant stabilized particles contracts in an adsorbing polymer solution is contrary to the usual considerations that the polymer adsorption may increase the effective size of

hard-wall particles. As is clearly shown in Figure 2, the main effect of adding amine-PEP into the colloidal solution is to change the value of $S_c(Q)$ in the small- Q region, whereas the peak position of $S_c(Q)$ (and hence the particle size) remains the same as that for the nonadsorbing colloid-PEP mixture.

With the three fitting parameters λ , σ and ϕ_c fixed, we were able to fit all the scattering data from the colloid-amine-PEP mixture samples having different ρ'_c and ρ'_p (12 samples in total) with only two free parameters: the interaction amplitudes P_d and P_a . However, the fitted values of P_d and P_a are found to be correlated, because the attraction tends to be cancelled out by the repulsion (i.e., the fitted P_d increases with P_a to a certain extent). To further differentiate the repulsive adsorption contribution to the colloidal interaction from the opposing attractive depletion contribution, we imposed a physical constraint to the depletion amplitude P_d . The fitted P_d as a function of the free polymer concentration, $\phi_p - (\phi_p)_a$, should behave the same as that for the nonadsorbing colloid-PEP mixtures, which has been measured recently with SANS.^{5,6} Then we need to know $\phi_p - (\phi_p)_a$ or, equivalently, the adsorption density ω_a (number of the adsorbed chains per colloidal particle) for a given total polymer concentration ρ'_p in the mixture. Unfortunately, this was not measured in our system. Theoretically, we have shown¹¹ that in the weak adsorption limit the effective volume fraction $(\phi_p)_a$ occupied by the adsorbed chains is proportional to both the total polymer and colloid concentrations. Therefore, we have¹¹

$$(\phi_p)_a = \alpha_1 \phi_p \phi_c \quad (13)$$

where α_1 is a proportionality constant which depends exponentially on the free energy of adsorption. In the fitting we simply treat α_1 as an extra parameter. It is found from the fitting that when we choose $\alpha_1 = 3.0$, P_d can be fitted to the same value as that for the corresponding colloid-PEP mixture, and at the same time the fitted P_a changes linearly with ω_a , as expected from eq 14, below.

Figure 5a shows the fitted P_d as a function of $\phi_p - (\phi_p)_a$ for the colloid-amine-PEP mixtures with $\rho'_c = 26.2$ wt % (circles) and $\rho'_c = 13.1$ wt % (squares). The dashed curve shows the measured P_d for the colloid-PEP mixture with $\rho'_c = 26.2$ wt %.^{5,6} It is seen that the fitted P_d first increases linearly with $\phi_p - (\phi_p)_a$ up to $\phi_p - (\phi_p)_a \approx 1$, and then it levels off. For a given $\phi_p - (\phi_p)_a$, P_d also depends upon ρ'_c . Recently, Lekkerkerker et al.^{4,36} pointed out that in the colloid-polymer mixtures the polymer number density n_p should be defined as $n_p = N_p/V_f$, where N_p is the total number of the polymer molecules and $V_f = \gamma(\phi_c)V$ is the free volume not occupied by the colloidal particles and their surrounding depletion zones. They have calculated $\gamma(\phi_c)$ as a function of the colloid volume fraction ϕ_c . As shown in Figure 5b, once $\phi_p - (\phi_p)_a$ is scaled by the calculated $\gamma(\phi_c)$,⁶ the two curves in Figure 5a collapse into a single master curve. The data are well described by the function $P_d = -0.054 + 0.178[(\phi_p - (\phi_p)_a)/\gamma] - 0.0245[(\phi_p - (\phi_p)_a)/\gamma]^2$ (solid curve), which is the same as that for the colloid-PEP mixture.^{5,6} The fitted function P_d consists of three terms. The small negative intercept indicates that there is a weak repulsive interaction between the soft surfactant shells of the colloidal particles, as discussed in the above. The linear term in P_d is due to the noninteracting polymer chains (an

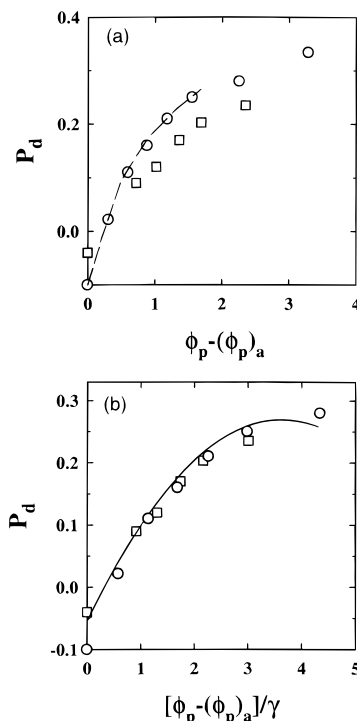


Figure 5. Fitted depletion amplitude P_d as a function of (a) $\phi_p - (\phi_p)_a$ and (b) $[\phi_p - (\phi_p)_a]/\gamma$ for the colloid-amine-PEP mixtures with $\rho'_c = 26.2$ wt % (○) and $\rho'_c = 13.1$ wt % (□). The dashed curve in (a) shows the fitted P_d for the colloid-PEP mixture with $\rho'_c = 26.2$ wt % . The solid curve in (b) is the fitted function $P_d = -0.054 + 0.178[(\phi_p - (\phi_p)_a)/\gamma] - 0.0245[(\phi_p - (\phi_p)_a)/\gamma]^2$.

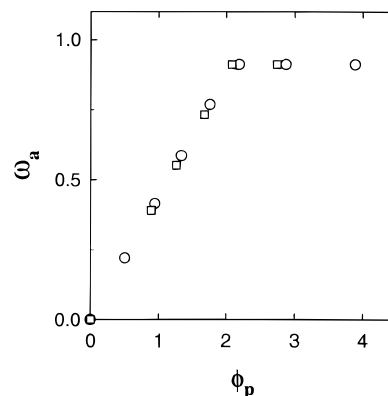


Figure 6. Fitted adsorption density ω_a as a function of ϕ_p for the colloid-amine-PEP mixture samples with $\rho'_c = 26.2$ wt % (○) and $\rho'_c = 13.1$ wt % (□).

ideal gas), and the polymer chain-chain interaction gives rise to the quadratic term.^{5,6}

It is also found from the fitting that eq 13 applies only to samples with small polymer concentrations. For the samples with $(\phi_p)_a/\phi_c > 6.25$, the fitted P_a would start to decrease if $(\phi_p)_a$ was forced to follow eq 13. This is unphysical, and we believe that P_a reaches a saturation limit. Therefore, we choose $P_a = 0.441$ (the saturation limit) for all the samples with higher polymer concentrations (see Table 1). With this value of P_a , the fitted values of P_d are still in good agreement with those for the corresponding colloid-PEP mixtures. We now can compute the adsorption density $\omega_a = (\phi_p)_a/[\phi_c(\lambda - 1)^3]$ (number of the adsorbed polymer chains per colloidal particle) using the fitted values of $(\phi_p)_a$, ϕ_c , and λ (see Table 1). Figure 6 shows the fitted ω_a for the mixture samples with $\rho'_c = 26.2$ wt % (circles) and $\rho'_c = 13.1$ wt % (squares). The fitted ω_a as a function of ϕ_p is consis-

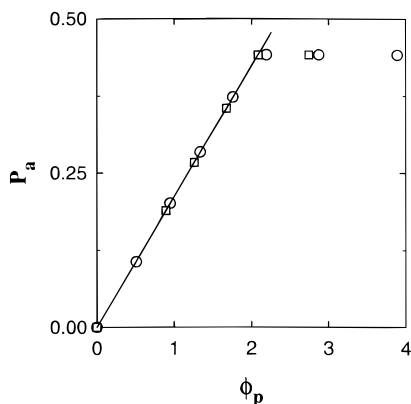


Figure 7. Fitted P_a as a function of ϕ_p for the colloid-amine-PEP mixtures with $\rho'_c = 26.2$ wt % (\circ) and $\rho'_c = 13.1$ wt % (\square). The solid line is the fitted linear function $P_a = 0.212\phi_p$.

tent with our expectation that in the weak adsorption limit the amount of the polymer adsorbed on the colloidal particles is proportional to the total amount of the polymer in the solution, and that the polymer adsorption will saturate when the total number of the polymer molecules becomes much larger than that of the colloidal particles. Note that for the mixture samples used in the experiment, the number ratio of the polymer molecules to the colloidal particles was varied from 0.5 to 6. It is seen from Figure 6 that the saturation value of ω_a is 0.91, which is not very large because the polymer adsorption is mitigated by the surfactant corona around the colloidal core. As mentioned in the above, the proportionality constant α_1 in eq 13 depends exponentially on the free energy of adsorption, which involves the adsorption energy ϵ between the end-functional group and the colloidal surface as well as the conformational entropy change for a free polymer chain to adsorb on the colloidal surface.¹¹ Using eqs 9 and 10 in ref 11 together with the fitted value of α_1 ($=3.0$), we find $\epsilon \approx 2.13k_B T$ which is close to our previously estimated value.¹¹

We now discuss the repulsive interaction amplitude P_a . Figure 7 shows the fitted P_a as a function of ϕ_p for the colloid-amine-PEP mixtures with $\rho'_c = 26.2$ wt % (circles) and $\rho'_c = 13.1$ wt % (squares). The solid line is the fitted linear function $P_a = 0.212\phi_p$ to the low concentration data. According to eq 7, the amplitude P_a should have the form

$$P_a = \frac{75\omega_a R_g}{2\sigma} = \frac{75\alpha_1}{4(\lambda - 1)^2} \phi_p \quad (14)$$

where we have used eq 13 to get the last equality. With the fitted values of α_1 ($=3.0$) and λ ($=2.9$), we find the prefactor $75\alpha_1/[4(\lambda - 1)^2] = 15.58$, which is approximately 74 times larger than the fitted value. The above fitting results thus reveal that the repulsive colloidal interaction due to the polymer adsorption can be well described by the exponential potential $\delta U_a(r) = P_a k_B T \exp[-2(r - o)/R_g]$, suggested by Dolan and Edwards (see eq 7). For the small colloidal particles, however, the interaction amplitude P_a is approximately 74 times smaller than the calculated value. In a recent surface force apparatus study, Ruths et al.³⁰ measured the force between two surfactant-coated mica surfaces across an adsorbing polymer solution. Their system was analogous to our colloid-amine-PEP mixture in that the mica surfaces were coated with similar surfactant molecules and immersed in the same polymer solution.

The only difference between the two systems was the adsorption substrate; one was a cylindrically curved large mica surface, and the other was a small calcium carbonate sphere. The measured surface-force curve was found to have the same exponential form as that shown in eq 6, but the magnitude of the force measured was larger than the value calculated by Dolan and Edwards. The two independent experiments therefore agree on the functional form of the repulsive interaction due to the polymer adsorption but not on the numerical value of the interaction amplitude. One plausible reason for the difference is that the two systems may have different adsorption densities because of the different adsorption substrates. Unfortunately, the adsorption density of amine-PEP is not known for either of the systems.

Another possibility is that in getting eq 6 we have invoked the Derjaguin approximation, which is valid only when the gap distance between two colloidal spheres is much smaller than the radius of the spheres.²⁸ For our mixture samples, however, the polymer molecules are larger than the colloidal particles, and therefore the Derjaguin approximation is not strictly applicable. In the calculation of the free energy $f(z)$ shown in Figure 1, Dolan and Edwards²⁷ have assumed that the adsorbed polymer chains are confined in between two parallel plates. When a polymer chain is attached to a small colloidal particle rather than a large flat surface, it can adopt more random-walk configurations and therefore has less resistance to the approach of other colloidal particles. As a result, the repulsion amplitude in eq 6 is overestimated, and thereby P_a in eq 7 becomes larger than its actual magnitude. In the above argument, we have assumed that the functional form of the interaction potential does not change very much when the particle size becomes comparable with the interaction range. In fact, one might even ask whether the theoretical calculation of the interaction between two parallel plates is relevant at all to the measured interaction potential between two small colloidal particles. The present scattering experiment together with the surface-force measurements suggest that for our colloid-amine-PEP mixtures, in which the range of the polymer-induced interactions is comparable with the particle size, the calculated functional form of the interaction potential is still applicable but the interaction amplitude needs to be modified. This conclusion is further supported by our recent study of the depletion interaction in the nonadsorbing colloid-PEP mixture.^{5,6}

It should be pointed out that, in the above data analysis, we have assumed that the colloidal particles are uniform in size and have considered only the polymer-induced interactions between the particles. In principle, the polydispersity in particle size and a small amount of surfactant aggregates in the mixture could also introduce depletion attractions, which may cause some degree of fractionation or association in the pure colloidal suspension.^{37,38} However, because the size difference between the colloidal particles is small and the polymer molecules are much larger than the surfactant aggregates, the depletion attraction due to these effects should be very weak compared with the polymer-induced interactions, and therefore it is unlikely to affect our data analysis. This argument is further supported by the following facts. (i) We did not observe any substantial amount of attraction in the measured $S_c(Q)$ for the pure colloidal samples. As shown in Figure

2, the measured $S_c(Q)$ for the pure colloidal suspension can be well described by a hard core potential plus a weak repulsive tail. (ii) Because the colloidal parameters are the same for each series of mixture samples with the same ϕ_c , the effects seen in Figures 2 and 3 are solely due to the addition of the polymer into the colloidal suspension.

V. Conclusion

We have used the small-angle neutron scattering technique to study the interaction between the colloidal particles when they are suspended in an adsorbing polymer solution. The colloidal particles used in the study were sterically stabilized CaCO_3 nanoparticles, and the polymer used was the end-functionalized poly(ethylene-propylene) (PEP). By matching the scattering length density of the solvent (decane) with that of the polymer, we measured the partial structure factor $S_c(Q)$ of the colloidal particles. The scattering results from the colloid-functionalized-PEP mixture are compared with those from the colloid-unfunctionalized-PEP mixture. It is found that the end-functionalized PEP molecules partition themselves between the bulk solution and the adsorbed state. The free polymer molecules in the solution introduce a depletion attraction between the colloidal particles, but the magnitude of the attraction is reduced considerably by the adsorbed polymer chains on the colloidal surfaces.

To quantitatively characterize the colloidal interaction in the polymer solution, we calculated the colloidal structure factor $S_c(Q)$ using an effective interaction potential $U(r)$, which includes both the depletion attraction and the repulsion due to the polymer adsorption. The calculated $S_c(Q)$ is found to fit the scattering data well. The fitting results suggest that the depletion attraction between the colloidal particles in the end-functionalized PEP solution behaves the same as that in the unfunctionalized PEP solution. It is found that the repulsive colloidal interaction due to the polymer adsorption can be well described by the exponential potential $\delta U_a(r) = P_a k_B T \exp[-2(r-\sigma)/R_g]$, suggested by Dolan and Edwards. However, the fitted interaction amplitude P_a is found to be approximately 74 times smaller than the calculated value for the interaction between two large parallel plates. Furthermore, the fitted P_a is found to increase linearly with the polymer concentration and reaches a saturation value at higher polymer concentrations. Because the direct interaction between the end-functional group of the polymer molecule and the polar core of the particle is mitigated by the surfactant corona around the particle, the polymer adsorption in the mixture samples is found to be weak. In this weak adsorption limit, we find that the adsorption energy between the polymer end-group and the colloidal surface is $\sim 2.1 k_B T$, and the maximum number of the adsorbed polymer chains per colloidal particle is approximately 1. The experiment clearly demonstrates the effectiveness of using unfunctionalized and end-functionalized polymers to control the colloidal interaction. With the ability of tailoring the microscopic interaction between the colloidal particles, one can control the macroscopic phase properties of many colloid-polymer mixtures, which are of direct interest to industries.

Acknowledgment. We have benefitted from useful discussions with J. S. Huang, T. A. Witten, P. Pincus, and Z.-G. Wang. We thank D. Schneider for his assistance with the SANS measurements and acknowledge the Brookhaven National Laboratory for granting neutron beam times. This work was supported by the National Aeronautics and Space Administration under Grant Nos. NAG3-1613 and NAG3-1852.

References and Notes

- (1) Russel, W. B.; Saville, D. A.; Schowalter, W. R. *Colloidal Dispersions*; Cambridge University Press: Cambridge, U. K., 1989.
- (2) Asakura, S.; Oosawa, F. *J. Chem. Phys.* **1954**, *22*, 1255.
- (3) Gast, A. P.; Hall, C. K.; Russel, W. B. *J. Colloid Interface Sci.* **1983**, *96*, 251.
- (4) Lekkerkerker, H. N. W.; *et al. Europhys. Lett.* **1992**, *20*, 559.
- (5) Ye, X.; Narayanan, T. Tong, P.; Huang, J. *Phys. Rev. Lett.* **1996**, *76*, 4640.
- (6) Ye, X.; *et al. Phys. Rev.* **1996**, *54*, 6500.
- (7) Napper, D. H. *Polymeric Stabilization of Colloidal Dispersions*; Academic Press: New York, 1983.
- (8) *Colloid-Polymer Interactions*; Dubin, P., Tong, P., Eds.; ACS Symposium Series 532; American Chemical Society: Washington, DC, 1993.
- (9) Vincent, B. *Adv. Colloid Interface Sci.* **1974**, *4*, 193.
- (10) Stuart, M. A. C.; Cosgrove, T.; Vincent, B. *Adv. Colloid Interface Sci.* **1986**, *24*, 143.
- (11) Carvalho, B. L.; *et al. Macromolecules* **1993**, *26*, 4632.
- (12) Markovic, I.; *et al. Colloid Polym. Sci.* **1984**, *262*, 648.
- (13) Markovic, I.; Ottewill, R. H. *Colloid Polym. Sci.* **1986**, *264*, 65.
- (14) O'Sullivan, T. P.; Vickers, M. E. *J. Appl. Crystallogr.* **1991**, *24*, 732.
- (15) Mays, J.; Hadjichristidis, N.; Fetters, L. J. *Macromolecules* **1984**, *17*, 2723.
- (16) May, J.; Fetters, L. J. *Macromolecules* **1989**, *22*, 921.
- (17) Davidson, N. S.; *et al. Macromolecules* **1987**, *20*, 2614.
- (18) Tong, P.; Witten, T. A.; Huang, J. S.; Fetters, L. J. *J. Phys. (Paris)* **1990**, *51*, 2813.
- (19) Nierlick, M.; Boue, F.; Lapp, A.; Oberthur, R. *Colloid Polym. Sci.* **1985**, *263*, 955.
- (20) Hansen, J.-P.; McDonald, I. R. *Theory of simple liquids*, 2nd ed.; Academic Press: London, 1991.
- (21) Vrij, A. *Pure Appl. Chem.* **1976**, *48*, 471.
- (22) Alexander, S. *J. Phys. (Paris)* **1977**, *38*, 977.
- (23) de Gennes, P. G. *Macromolecules* **1980**, *13*, 1069.
- (24) Milner, S. T.; Witten, T. A.; Cates, M. E. *Europhys. Lett.* **1988**, *5*, 413.
- (25) Milner, S. T.; Witten, T. A.; Cates, M. E. *Macromolecules* **1988**, *21*, 2160.
- (26) Milner, S. T. *Science* **1991**, *251*, 905.
- (27) Dolan, A. K.; Edwards, S. F. *Proc. R. Soc. London A.* **1974**, *337*, 509.
- (28) Israelachvili, J. *Intermolecular and Surface Forces*, 2nd ed.; Academic Press: London, 1992.
- (29) Gee, M.; Tong, P.; Israelachvili, J.; Witten, T. *J. Chem. Phys.* **1990**, *93*, 6057.
- (30) Ruths, M.; Yoshizawa, H.; Fetters, L. J.; Israelachvili, J. *Macromolecules* **1996**, *29*, 7193.
- (31) Wertheim, M. *Phys. Rev. Lett.* **1963**, *8*, 321.
- (32) Thiele, E. *J. Chem. Phys.* **1963**, *38*, 1959.
- (33) Ashcroft, N. W.; Lekner, J. *Phys. Rev.* **1966**, *154*, 83.
- (34) Gast, A. P.; Leibler, L. *Macromolecules* **1986**, *19*, 686.
- (35) Milner, S. T. *Europhys. Lett.* **1988**, *7*, 695.
- (36) Ilett, S. M. Orrock, A.; Poon, W.; Pusey, P. *Phys. Rev. E* **1995**, *51*, 1344.
- (37) Bibette, J.; Roux, D.; Nallet, F. *Phys. Rev. Lett.* **1990**, *65*, 2470.
- (38) Bibette, J. *J. Colloid Interface Sci.* **1991**, *147*, 474.